The current issue and full text archive of this journal is available on Emerald Insight at:
https://www.emerald.com/insight/2633-6596.htm

Received 26 October 2022
Revised 11 December 2022
Accepted 1 January 2023

A combined vertical accuracy compensation method for automatic drilling and riveting of aircraft panels with variable curvatures

Junshan Hu
College of Mechanical and Electrical Engineering, Nanjing University of Aeronautics and Astronautics, Nanjing, China and Technical Center, State-operated Wuhu Machinery Factory, Wuhu, China
Jie Jin and Yueya Wu
College of Mechanical and Electrical Engineering, Nanjing University of Aeronautics and Astronautics, Nanjing, China
Shanyong Xuan
Technical Center, State-operated Wuhu Machinery Factory, Wuhu, China, and
Wei Tian
College of Mechanical and Electrical Engineering, Nanjing University of Aeronautics and Astronautics, Nanjing, China

Abstract

Purpose – Aircraft structures are mainly connected by riveting joints, whose quality and mechanical performance are directly determined by vertical accuracy of riveting holes. This paper proposed a combined vertical accuracy compensation method for drilling and riveting of aircraft panels with great variable curvatures.

Design/methodology/approach – The vertical accuracy compensation method combines online and offline compensation categories in a robot riveting and drilling system. The former category based on laser ranging is aimed to correct the vertical error between actual and theoretical riveting positions, and the latter based on model curvature is used to correct the vertical error caused by the approximate plane fitting in variable-curvature panels.

Findings – The vertical accuracy compensation method is applied in an automatic robot drilling and riveting system. The result reveals that the vertical accuracy error of drilling and riveting is within 0.4°, which meets the requirements of the vertical accuracy in aircraft assembly.

© Junshan Hu, Jie Jin, Yueya Wu, Shanyong Xuan and Wei Tian. Published in *Journal of Intelligent Manufacturing and Special Equipment*. Published by Emerald Publishing Limited. This article is published under the Creative Commons Attribution (CC BY 4.0) licence. Anyone may reproduce, distribute, translate and create derivative works of this article (for both commercial and non-commercial purposes), subject to full attribution to the original publication and authors. The full terms of this licence may be seen at http://creativecommons.org/licences/by/4.0/legalcode

This work is financially supported by the National Key Research and Development Program of China (Grant No. 2019YFB1310103), Anhui Key research and development project (Grant No. 202203a05020039), China Postdoctoral Science Foundation (Grant No. 2022M720939) and Jiangsu Key Laboratory of Precision and Micro-Manufacturing Technology Foundation (Grant No. ZAA20003-05). Moreover, the authors would like to acknowledge the editors and the anonymous referees for their insightful comments.

Journal of Intelligent Manufacturing and Special Equipment
Vol. 4 No. 1, 2023
pp. 64-81
Emerald Publishing Limited
e-ISSN: 2633-660X
p-ISSN: 2633-6596
DOI 10.1108/JIMSE-10-2022-0019

Originality/value – The proposed method is suitable for improving the vertical accuracy of drilling and riveting on panels or skins of aerospace products with great variable curvatures without introducing extra measuring sensors.

Keywords Automatic drilling and riveting, Vertical accuracy compensation, Online and offline correction, Variable-curvature panels

Paper type Research paper

1. Introduction

Nowadays aircraft components such as fuselage skins, wing panels and stringers are dominantly connected by riveting in assembly, thus the riveting quality directly determines the mechanical performance of assembly structures (Li *et al.*, 2022). Commonly the riveting joints are achieved by drilling with subsequent riveting process, and the vertical accuracy of riveting holes has always been the research focus in the aerospace manufacturing industry (Gao *et al.*, 2017; Mei *et al.*, 2018; Lee and Shiou, 2010). Studies have shown that if the vertical accuracy of the riveting hole fails to meet the vertical precision, the connector would be inclined to produce bending stress, and the structural strength is greatly reduced (Prakash *et al.*, 2016). When the inclination angle of the fastener along the direction of the external load is greater than 2°, the fatigue life is reduced by about 47%. If the inclination angle is greater than 5°, the fatigue life is reduced by 95% (Mei *et al.*, 2018). It can be concluded that the vertical accuracy of drilling and riveting is crucial for the aircraft quality and service life.

In aircraft assembly, the drilling and riveting processes are often achieved by automatic drilling and riveting equipments (Hu *et al.*, 2022). After decades of development, the drilling and riveting equipments for aviation products has been able to complete a series of functions such as positioning, pose adjustment, drilling, rivets feeding, riveting, inspecting, etc (Jin *et al.*, 2022). For example, the G-series automatic drilling and riveting system developed by GEMCOR (Rummell, 2000) and the robot drilling and riveting system cell developed by Broetje-Automation GmbH (Wang *et al.*, 2010; Alici and Shirinzadeh, 2005) are the representatives. In order to ensure the vertical accuracy of riveting holes, these automatic drilling and riveting system need to employ vertical accuracy compensation technology to adjust the vertical accuracy of the tool axis to ensure the normal vector of riveting holes in workpiece surface.

Actually a certain degree of progress has been made in the vertical accuracy compensation technology in automatic drilling and riveting field. The vertical accuracy compensation technology for automatic drilling can be divided into mechanical contact type, eddy current type, laser non-contact type and visual non-contact type according to the measurement method (Zhang *et al.*, 2018). The mechanical contact type generally uses a contact linear displacement sensor for surface measurement, and it has a good effect on the measurement of the plane normal vector with advantages of high measurement accuracy and low budget cost (Jin *et al.*, 2022). The vertical accuracy of riveting holes in workpiece surfaces which possess plain and constant curvature are easily achieved by this kind of compensation technology in aerospace assembly (Lee and Shiou, 2010; Cao *et al.*, 2018). Universite Lund in Sweden realizes the pose correction of the robot's end effector using a pressure sensor arranged around the pressure foot (Olsson *et al.*, 2010), which also belongs to mechanical contact type. The eddy current type adopts eddy current sensors which could measure the surface of metal workpieces and obtain the distance through the change signal of eddy current intensity, so as to calculate the normal vector of the measured surface (Su *et al.*, 2017). The laser non-contact type uses laser displacement sensors for non-contact measurement, which has the characteristics of high measurement accuracy, non-direct contact with the surface of the workpiece and high safety (Cao *et al.*, 2018; Lee and Shiou, 2011). The Electroimpact company has studied the error correction compensation technology based on

linear displacement sensors, which is then integrated into the ONCE robot automatic drilling system (DeVlieg *et al.*, 2002) and the automated wing drilling system for the A380-GRAWDE (Hogan *et al.*, 2003). The visual non-contact type is difficult to guarantee vertical accuracy requirements in complex operating environments due to the factors such as shooting angle, light condition, processing algorithm, etc (Tian *et al.*, 2013).

The above methods can obtain high-precision normal measurement results when measuring planes of workpieces have approximately or exactly constant curvature surfaces (Tian *et al.*, 2013). But it is difficult to meet the perpendicularity precision of riveting holes in the cases when the measured normal vectors do not coincide with the actual normal vectors because of the variable curvature surface. In this research, a vertical accuracy compensation method based on both online calibration and offline prediction is proposed. The proposed method first corrects the normal vector of drilling and riveting points online using a fitting the plane normal vector with data of laser ranging. Then it predicts the inherent theoretical error of normal vector offline caused by fitting curved surfaces with plane ones. These two kinds of errors are quantified and employed to adjust the pose of the end effector so as to realize high vertical accuracy for the automatic drilling and riveting of the variably curved surface.

2. Establishment of vertical accuracy compensation method

2.1 Problem configuration

The verticality error limit of riveting holes in aircraft panel assembly is within ±0.5°. Due to manufacturing errors in workpieces, calibration errors of coordinate systems, and the local deformation introduced by gravity and clamping forces, the actual surface of the workpiece is different from the theoretical model when automatic drilling and riveting equipments are employed to conduct drilling and riveting operations (Hu *et al.*, 2022). The pose of robot machining planned offline according to the three dimensional (3D) theoretical models is unable to satisfy the vertical accuracy of riveting holes. Therefore, it is necessary to adjust the pose of the end effector to make the drilling and riveting axis perpendicular to the workpiece surface. In order to redefine the normal vector of the drilling position for drilling and riveting equipments, a fitted plane on the drilling spot of the actual workpiece is used for vertical accuracy compensation to replace the theoretical normal vector from 3D models in consideration of that the small area around the drilling spot is approximately regarded as a plane. However, it is not the case for a cured surface of the aircraft panel with small variable curvature radiuses. There is a deflection angle between the fitted and the actual normal vectors when plane fitting is employed to obtain the normal vector of workpiece surface with variable curvatures. Thus, the vertical accuracy of drilling and riveting holes is not only corrected by online compensation but also further amended by offline compensation according to the theoretical model of the workpiece surface.

2.2 Vertical accuracy online compensation based on laser ranging

Before the drilling operation, it is necessary to modify the posture of the end effector so that the axis of the tool is perpendicular to the surface of the workpiece, and the verticality of the drilling hole is guaranteed. The workflow of the laser non-contact normal measurement for online vertical accuracy compensation of drilling on workpiece with variable curvature surface is shown in Figure 1. Firstly, in order to determine the pose of the robot end effector, four laser displacement sensors are employed to measure the distance of the curved surface to obtain the position information of the four projection points on the curved surface, as shown in Figure 2, and the plane is fitted by the plane fitting algorithm. Then the actual drilling pose is updated by using the normal vector of the fitted plane as that of the drilling hole. Finally, the end effector adjusts its posture to complete the vertical accuracy compensation.

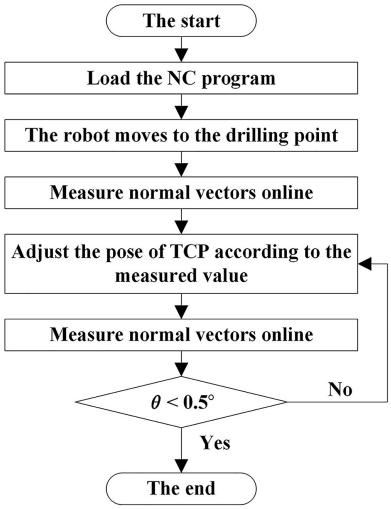

Figure 1. The workflow of the vertical accuracy online compensation based on laser ranging

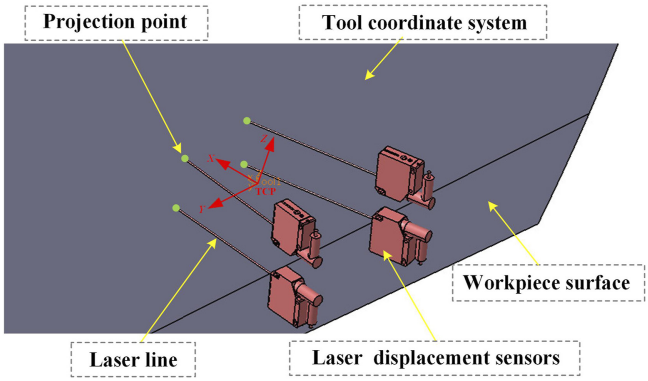

Figure 2. Projection points of laser displacement sensors

2.2.1 Calibration of displacement sensors. The position of the laser displacement sensor and the specific location of the workpiece surface in the tool coordinate system can be obtained through the sensor calibration. As shown in Figure 3, the tool center point (TCP) coordinate system is located at the drilling tool tip. There are six axes in the TCP, among which X, Y, Z are translational axes and A, B, C are rotational axes around them as presented in Figure 3a. The laser displacement sensors (Baumer CH-8501) are installed around the press foot of the end effector as presented in Figure 3b.

The measuring instrument used in the calibration is an API-T3 laser tracker, and the aided calibration tool is a standard calibration plate. The standard calibration plate is fixed in a suitable distance directly in front of the end effector, that is, the plate and the end effector under multiple measurement poses should be within the measurable range of the API-T3 laser tracker, as shown in Figure 4. Meanwhile, the base coordinate, the flange coordinate and the tool coordinate are also established. The robot base coordinate is established by rotating axes A1 and A2 under the laser tracker coordinate system. The flange coordinate FLAN is established by reading the robot flange coordinate (x, y, z, A, B, C) through the robot control

panel. The tool coordinate TCP is established by placing the target ball on the spindle handle equipped with the target holder, that is, the main spindle axial is measured by feeding a certain distance along its axial direction, and this spindle axis is regarded as the X-axis of TCP. The Y-axis of TCP is the normal direction of the plane determined by the Z-axis of the robot coordinate system and the X-axis of TCP. The position at a distance of 10.0 mm in front of the pressure foot along the main axis is taken as the origin. The TCP of the end effector in the flange coordinate FLAN is established in SpatialAnalyzer software environment. By reading the matrix relationship ${}^{TCP}_{FLAN}T$ between the tool coordinate system and the flange coordinate system and inputting it into the robot control pane, TCP of the robot is finally created in the robot control system.

After establishment of the coordinate systems, the laser tracker is employed to measure the surface of the standard calibration plate in the tool coordinate TCP. According to the measured point cloud data, the plane equation of the standard calibration plate is fitted by:

$$ax + by + cz = d \tag{1}$$

where a, b, c are three components of the plane normal unit vector in the tool coordinate system, respectively, and d is the distance between the origin of the tool coordinate TCP and the plane.

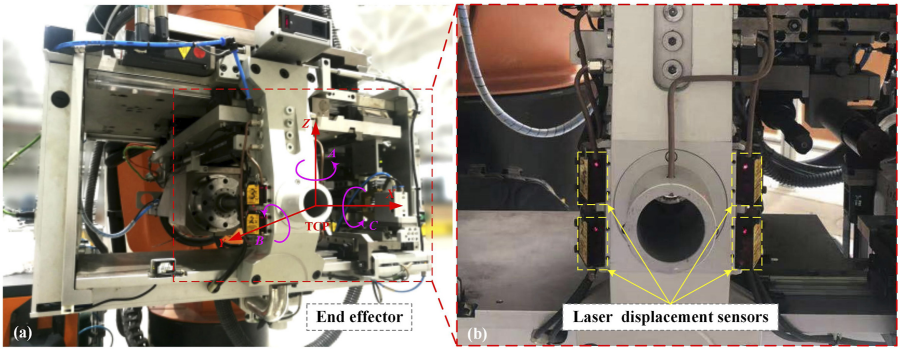

Figure 3.
The end effector used for drilling and riveting: (a) tool coordinate system (TCP) of end effector and (b) laser displacement sensors on end effector

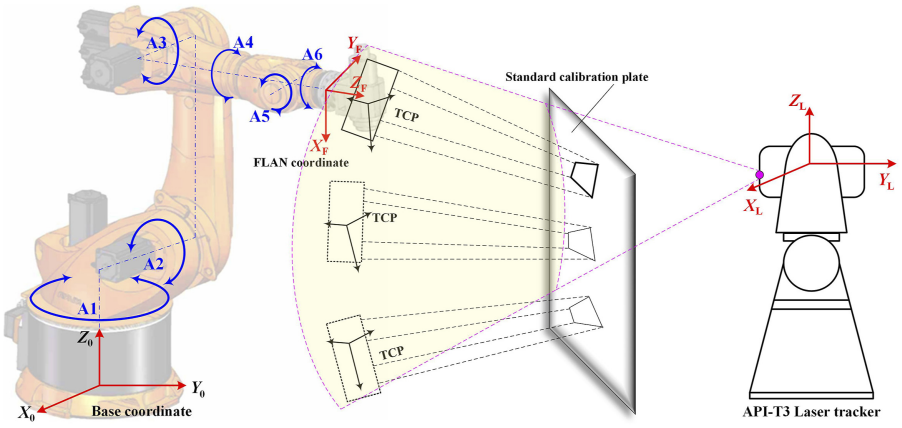

Figure 4.
The establishment of TCP system through coordinate transformation by calibration

The pose of the four laser displacement sensors in the tool coordinate TCP is supposed to be $(x_i, y_i, z_i, m_i, n_i, p_i)$, and the measured value is l_i, in which $i \in (1, 2, 3, 4)$, then the intersection point between the projected light of the laser displacement sensor and the standard calibration plate can be expressed by:

$$\begin{pmatrix} x_i' \\ y_i' \\ z_i' \end{pmatrix} = \begin{pmatrix} x_i \\ y_i \\ z_i \end{pmatrix} + l_i \begin{pmatrix} m_i \\ n_i \\ p_i \end{pmatrix} = \begin{pmatrix} x_i + l_i m_i \\ y_i + l_i n_i \\ z_i + l_i p_i \end{pmatrix} \tag{2}$$

By substituting the coordinates of the intersection points into the plane Equation (1), there is:

$$a(x_i + l_i \mathrm{m}_i) + b(y_i + l_i n_i) + c(z_i + l_i p_i) = d \tag{3}$$

Equation (3) can be put in the following format:

$$ax_i + by_i + cz_i + al_i \mathrm{m}_i + bl_i n_i + cl_i p_i = d \tag{4}$$

There are six unknown parameters in Equation (4), namely $(x_i, y_i, z_i, m_i, n_i, p_i)$. They are exactly the position and direction vector of the laser displacement sensor that needs to be calibrated. By adjusting the pose of the robot end effector several times (within the measurement range of the laser displacement sensors), multiple sets of the laser displacement sensor values are obtained to create six equations to solve the unknown parameters in Equation (4). The equation group is expressed as follows:

$$\begin{cases} a_1 x_i + b_1 y_i + c_1 z_i + a_1 l_i^1 m_i + b_1 l_i^1 n_i + c_1 l_i^1 p_i = d_1 \\ a_2 x_i + b_2 y_i + c_2 z_i + a_2 l_i^2 m_i + b_2 l_i^2 n_i + c_2 l_i^2 p_i = d_2 \\ a_3 x_i + b_3 y_i + c_3 z_i + a_3 l_i^3 m_i + b_3 l_i^3 n_i + c_3 l_i^3 p_i = d_3 \\ a_4 x_i + b_4 y_i + c_4 z_i + a_4 l_i^4 m_i + b_4 l_i^4 n_i + c_4 l_i^4 p_i = d_4 \\ a_5 x_i + b_5 y_i + c_5 z_i + a_5 l_i^5 m_i + b_5 l_i^5 n_i + c_5 l_i^5 p_i = d_5 \\ a_6 x_i + b_6 y_i + c_6 z_i + a_6 l_i^6 m_i + b_6 l_i^6 n_i + c_6 l_i^6 p_i = d_6 \end{cases} \tag{5}$$

where l_i^j is the jth group testing value of the ith laser displacement sensor, $j \in (1, 2, 3, 4, 5, 6)$. Equation (5) can be expressed in the form of a homogeneous linear equation group:

$$\begin{bmatrix} a_1 & b_1 & c_1 & a_1 l_i^1 & b_1 l_i^1 & c_1 l_i^1 \\ a_2 & b_2 & c_2 & a_2 l_i^2 & b_2 l_i^2 & c_2 l_i^2 \\ a_3 & b_3 & c_3 & a_3 l_i^3 & b_3 l_i^3 & c_3 l_i^3 \\ a_4 & b_4 & c_4 & a_4 l_i^4 & b_4 l_i^4 & c_4 l_i^4 \\ a_5 & b_5 & c_5 & a_5 l_i^5 & b_5 l_i^5 & c_5 l_i^5 \\ a_6 & b_6 & c_6 & a_6 l_i^6 & b_6 l_i^6 & c_6 l_i^6 \end{bmatrix} \begin{bmatrix} x_i \\ y_i \\ z_i \\ m_i \\ n_i \\ p_i \end{bmatrix} = \begin{bmatrix} d_1 \\ d_2 \\ d_3 \\ d_4 \\ d_5 \\ d_6 \end{bmatrix} \tag{6}$$

According to Equation (6), the position vectors and direction vectors of the four laser displacement sensors can be obtained. In calibration process, the collected calibration data are generally much larger than six groups to ensure calibration accuracy, and the calibration data are solved by the least square method to finally determine the values of $x_i, y_i, z_i, m_i, n_i, p_i$ for the four laser displacement sensors in the tool coordinate TCP.

2.2.2 Online correction of drilling and riveting verticality. The positions of four projection points in the tool coordinate system TCP can be obtained by Equation (2). A plane and its normal vector $\boldsymbol{N} = (i, j, k)$ can be obtained by plane fitting through four projection points of laser sensors with the least square fitting method. The drilling pose of the robot end effector is resolved according to the fitted normal vector.

In order to adjust the pose of the robot end effector according to the fitted normal vector, it is necessary to recalculate the posture of TCP in the robot base coordinate system. Therefore, the normal vector of the fitting plane should be transferred from the tool coordinate system to the robot base coordinate system. $\boldsymbol{T}$ is the posture of the current TCP in the robot base coordinate system, so the transformation relationship can be expressed by:

$$\boldsymbol{N}' = \boldsymbol{T}\boldsymbol{N} \tag{7}$$

According to the theory of robot kinematics, the attitude of the tool coordinate system can be expressed as:

$$\boldsymbol{F} = \begin{bmatrix} \boldsymbol{n_x} & \boldsymbol{o_x} & \boldsymbol{a_x} \\ \boldsymbol{n_y} & \boldsymbol{o_y} & \boldsymbol{a_y} \\ \boldsymbol{n_z} & \boldsymbol{o_z} & \boldsymbol{a_z} \end{bmatrix} \tag{8}$$

wherein $\boldsymbol{n}$, $\boldsymbol{o}$ and $\boldsymbol{a}$ are orthogonal unit vectors. The relationship $\boldsymbol{n} = N'$ (N' is the identity matrix) is established to ensure that the X-axis of the calculated tool coordinate TCP is consistent with the normal vector of the fitted plane. The relation $\boldsymbol{o} = (-\boldsymbol{n}_y, \boldsymbol{n}_x, 0)$ is made to achieve the relationship in which the Y-axis of the coordinate system is perpendicular to the X-axis and parallel to the ground. So the vector $\boldsymbol{a}$ is:

$$\boldsymbol{a} = \boldsymbol{n} \times \boldsymbol{o} \tag{9}$$

Therefore, the matrix expression of the tool coordinate system TCP in the robot base coordinate system can be calculated, and then it converts to Euler angle (A, B, C) by successively revolving around the Z-Y-X axes. The posture of the end effector can be adjusted to complete the normal vector correction.

2.3 Vertical accuracy offline compensation based on model curvature

As mentioned earlier, the online compensation based on laser ranging above are suitable for operating of panels with plain surface or consistent curvature, but it is not the case for those workpiece with variable curvatures. The main reason that the laser non-contact normal measurement method has a large error in the measurement of surfaces with variable curvature is the existence of the inherent theoretical error. As the side projection shown in Figure 5, due to the variation of the surface curvature, the four projection points on the surface are asymmetric with the center of the hole to be drilled. Therefore, the plane normal fitted by the 4 projection points cannot coincide with the theoretical normal, and there is a theoretical deviation angle. Obviously, the deviation angle is related to the variation degree of the curvature in the surface. Hence, there is a large inherent theoretical error in using the laser non-contact method to compensate for the vertical accuracy of the variable curvature surface.

In order to obtain the inherent theoretical error, the vertical accuracy offline compensation method is proposed based on the simulation of the laser non-contact normal accuracy compensation in 3D theoretical model. The deflection angle θ between the X-axis of the tool coordinate TCP and the normal direction of the point to be measured in the simulation environment is the predicted value of the theoretical error. The workflow of the vertical accuracy offline compensation method is presented in Figure 6. Firstly, the vertical accuracy compensation process is simulated according to the actual situation in DELMIA software,

and the inherent theoretical error is predicted as the declination angle for vertical accuracy compensation. Secondly, the inherent theoretical error and point information are input into the drilling and riveting system, and the robot end effector is moved to the point to be drilled. The online normal accuracy compensation process is implemented until the angle between the previous measured normal direction and the present one is less than 0.5°. Finally, the tool coordinate TCP is compensated with the predicted theoretical inherent error, and the pose of the end effector is adjusted according to the declination angle of the normal vector.

2.3.1 Normal vector declination of drilling and riveting. In the actual measurement, the laser non-contact normal measurement process is as follows: projection point acquisition – plane fitting – normal direction acquisition – robot pose adjusting. In the simulation process, the plane fitting algorithm should be exactly the same as the algorithm in the actual measurement environment. The least-square method is used as the plane fitting algorithm in this research (Lee and Shiou, 2011).

After completing the simulation of the laser non-contact normal measurement process in DELMIA software, the X-axis of the tool coordinate TCP coincides with the plane normal vector fitted by the four projection points, and at this time, the relationship between the theoretical normal of the surface and the tool coordinate pose is shown in Figure 7. $T - XYZ$ is the tool coordinate system. RT is the intersection line of the coordinate plane XTY and coordinate plane XTZ. The vector $\overrightarrow{TF}$ is the theoretical normal vector of the workpiece surface. θ is the angle between the vector $\overrightarrow{TF}$ and the X-axis of the tool coordinate system, called the theoretical declination. $\overrightarrow{TN}$ is the projection vector of the vector $\overrightarrow{TF}$ on the

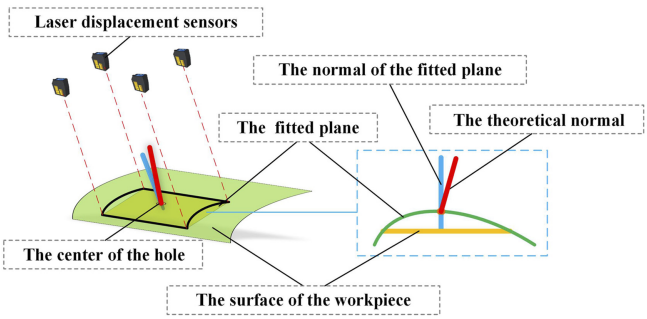

Figure 5. The principle diagram of theoretical error analysis

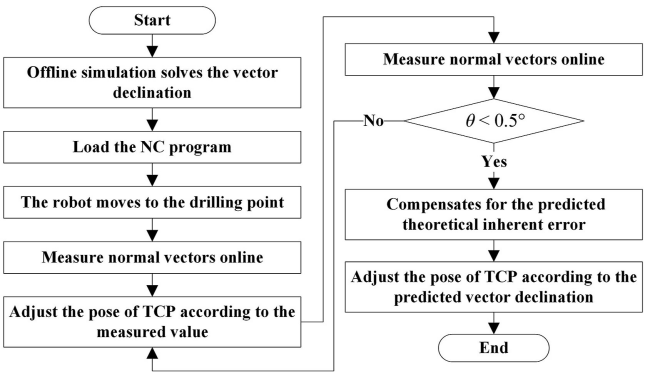

Figure 6. The workflow of vertical accuracy offline compensation based on model curvature

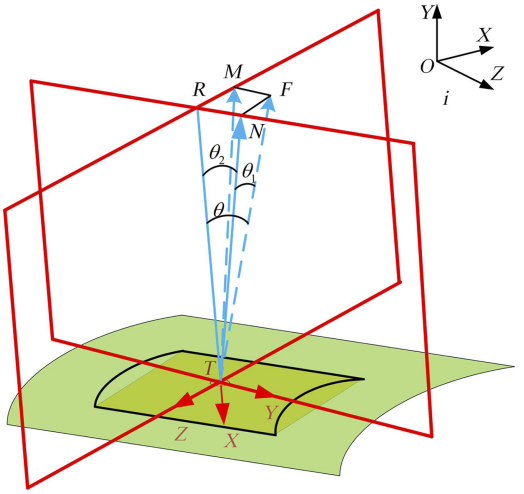

Figure 7.
Relationship between tool coordinate system attitude and theoretical normal

coordinate plane XTY. $\overrightarrow{TM}$ is the projection vector of vector $\overrightarrow{TF}$ on the coordinate plane XTZ. θ_1 is the angle between the vector $\overrightarrow{TF}$ and the vector $\overrightarrow{TN}$. θ_2 is the angle between the vector $\overrightarrow{TN}$ and the X-axis of the tool coordinate system. The inherent theoretical error can be expressed by the theoretical deflection angle θ. Considering the pose adjustment calculation of the robot end effector in the actual process, θ_1 and θ_2 are used to represent the theoretical error. The derivations of θ_1 and θ_2 are determined as follows.

θ_1 is the angle between the vector $\overrightarrow{TN}$ and the coordinate plane XTY. It can be expressed as:

$$\theta_1 = \arcsin \frac{\overrightarrow{TF} \cdot \overrightarrow{m}}{|\overrightarrow{TF}| \cdot |\overrightarrow{m}|} \tag{10}$$

where $\overrightarrow{m}$ is the normal vector of the coordinate plane XTY, and $\frac{\overrightarrow{m}}{|\overrightarrow{m}|}$ can be expressed as the unit vector $\overrightarrow{k}$ of the Z-axis. Thus Equation (7) can be rewritten as:

$$\theta_1 = \arcsin \frac{\overrightarrow{TF}}{|\overrightarrow{TF}|} \cdot \overrightarrow{k} \tag{11}$$

The projection vector $\overrightarrow{TN}$ can be expressed as:

$$\overrightarrow{TN} = \overrightarrow{TF} \cos \theta_1 \tag{12}$$

θ_2 is the angle between the vector $\overrightarrow{TN}$ and the X-axis of the tool coordinate system, which can be expressed as:

$$\cos \theta_2 = \frac{\overrightarrow{TN}}{|\overrightarrow{TN}|} \cdot \overrightarrow{\tau} \tag{13}$$

From Equations (2), (3) and (4), there is:

$$\theta_2 = \arccos\left(\frac{\overrightarrow{TF}\cdot\vec{\tau}}{|\overrightarrow{TF}|\cos\left(\arcsin\frac{\overrightarrow{TF}}{|\overrightarrow{TF}|}\cdot\vec{k}\right)}\right) \tag{14}$$

2.3.2 Offline correction of normal vector declination. The purpose of the offline correlation of normal vector declination is to apply the inherent theoretical error to the pose adjustment of the end effector. The theoretical error angles θ_1 and θ_2 are input into the robot control system to realize the normal accuracy compensation for the panel surface with variable curvature after the online compensation based on laser ranging. Actually when online accuracy compensation is finished, the deviation between the tool coordinate system and the actual normal vector to be measured is approximately the same as that in the simulation, and the relationship between the pose of the tool coordinate system and the theoretical normal vector can be shown in Figure 7. The pose of the tool coordinate system based on θ_1 and θ_2 needs to be adjusted to make the X-axis coincide with the theoretical normal vector. The pose adjustment procedure is as follows:

The pose of the current tool coordinate system is supposed to be (X, Y, Z, A, B, C), thus the current pose is represented by the Euler angle transformation sequence as:

$$Euler(A, B, C) = Rot(z, C)Rot(y, B)Rot(x, A) \tag{15}$$

$$Rot(x, A) = \begin{bmatrix} 1 & 0 & 0 \\ 0 & cA & -sA \\ 0 & sA & cA \end{bmatrix} \tag{16}$$

$$Rot(y, B) = \begin{bmatrix} cB & 0 & sB \\ 0 & 1 & 0 \\ -sB0 & s00 & cB \end{bmatrix} \tag{17}$$

$$Rot(z, C) = \begin{bmatrix} cC & -sC & 0 \\ sC & cC & 0 \\ 0 & 0 & 1 \end{bmatrix} \tag{18}$$

where s denotes sine, and c represents cosine.

The current position of the tool coordinate system is kept unchanged to adjust the posture of the tool coordinate system. The tool coordinate system is rotated around its Z-axis by angle θ_2, and then it is rotated around its Y-axis by angle θ_1. The rotation matrix can be expressed as:

$$Rot(y, \theta_2)Rot(z, \theta_1) = \begin{bmatrix} c\theta_2 & 0 & s\theta_2 \\ 0 & 1 & 0 \\ -s\theta_2 & 0 & c\theta_2 \end{bmatrix} \begin{bmatrix} c\theta_1 & -s\theta_1 & 0 \\ s\theta_1 & c\theta_1 & 0 \\ 0 & 0 & 1 \end{bmatrix} = \begin{bmatrix} c\theta_2 c\theta_1 & -c\theta_2 s\theta_1 & s\theta_2 \\ s\theta_1 & c\theta_1 & 0 \\ -s\theta_2 c\theta_1 & s\theta_2 s\theta_1 & c\theta_2 \end{bmatrix} \tag{19}$$

By combining Equations (6) and (10), the final processing pose after two rotations can be expressed as:

$$Euler(A, B, C) = Rot(y, \theta_2)Rot(z, \theta_1) \tag{20}$$

The vertical accuracy compensation of the variable curvature surface is completed according to the above-mentioned adjustment process.

2.4 Error analysis of vertical accuracy compensation method

The vertical accuracy compensation method for surface with variable curvature is proposed in this research, and the error can be divided into online laser non-contact normal measurement error and offline theoretical prediction error. The online laser non-contact normal measurement error has been investigated in many literature studies, so only the offline prediction error is thoroughly analyzed here. The offline prediction error is mainly caused by the deviation between the irradiation point position of the laser displacement sensor on the workpiece and the actual irradiation point position in the offline simulation process (Lee and Shiou, 2011). The main factors that lead to the prediction error include the absolute robot positioning accuracy error and the robot end pose error. The X-axis of the tool coordinate system of the end effector is consistent with the normal direction of the online measurement after repeatedly online pose adjustments, so the pose error of the robot end can be ignored. The error introduced by the absolute positioning accuracy will be deeply analyzed.

In the actual normal measurement process, there is an error Δa which is called the absolute positioning accuracy of the robot between the actual position of the robot end and the theoretical position. As shown in Figure 8, θ is the deflection angle between the theoretical normal vector and the fitting normal vector through the simulation, and it is the inherent theoretical error angle predicted in the theoretical simulation environment. θ' is the deflection angle between the normal vector of the actual hole to be drilled and the fitting normal vector. It is the inherent theoretical error angle that actually exists. Due to the existence of the error Δa, the actual and the theoretical processing points are discordant in the actual drilling process, and there must be a difference between the inherent theoretical error angle θ predicted in the theoretical simulation and the actual inherent theoretical error angle θ'. Once the predicted inherent theoretical error angle θ is used to replace the actual inherent theoretical error angle θ', the predicted error angle $\Delta\theta$ appears:

$$\Delta\theta = \theta - \theta' \tag{21}$$

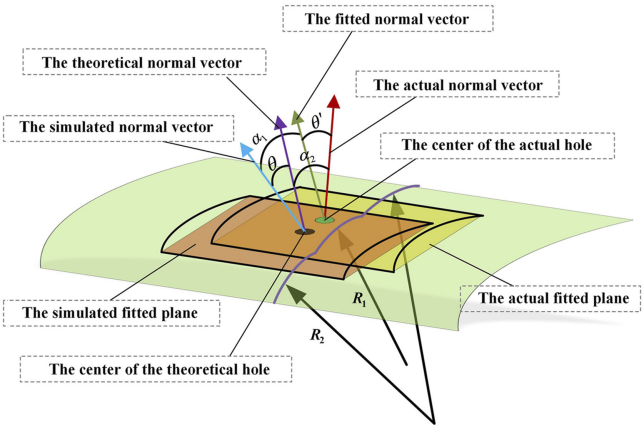

Figure 8.
Schematic diagram of error maximization analysis

In order to analyze the relationship among the curvature radius of the surface R, the absolute positioning accuracy of the robot Δa, the distance of the measured displacement from laser sensor L and the predicted angle error $\Delta\theta$, the limit thought is adopted to build the specific conditions when the predicted angle error $\Delta\theta$ reaches the maximum value. It is assumed that the maximum radius of curvature R_1 and the minimum radius of curvature R_2 exist in this curved surface, the radius difference of the curvature ΔR can be expressed as:

$$\Delta R = R_2 - R_1 \tag{22}$$

As shown in Figure 8, when the point to be measured is in the curved surface R_1 and the projection points of the laser displacement sensor on the workpiece are all in the curved surface R_2, the angle α_1 between the actual normal vector and the simulated normal vector reaches the minimum value and the angle α_2 between the normal vector of the actual hole and the normal vector of the theoretical hole reaches the maximum value. The predicted angle error $\Delta\theta$ reaches the maximum value. At this point, the value of $\Delta\theta$ is:

$$\Delta\theta = \alpha_2 - \alpha_1 \tag{23}$$

2.4.1 α_1 error analysis. The relationship among R, Δa, L and α_1 is established on condition that the radius of curvature R, the robot's absolute positioning accuracy Δa and the laser displacement sensor measuring point distance L keep unchanged. In the mathematical analysis model, the measurement area of the laser displacement sensor $R2$ is shown in Figure 9, where the radius of the measurement area is $R2$, and the center of the circle O is sensor. The straight line WV connected to the theoretical projection points in the two simulation cases. Assuming that the line segment WV is parallel to MN (WV // MN), and the line segment MN is the diameter of the R_2 circle. $W'V'$ is the straight line connected to the projection point in the actual measurement, and there is $|WV| = |W'V'| = L$. The straight line $V'D$ is through point V' and perpendicular to N. It intersects with WV and MN at points H and D, respectively. The auxiliary lines OV, VV', OV' and auxiliary angle β are created in the model. When the absolute positioning error Δa occurs along the VW direction, α_1 reaches the maximum value, which is:

$$HV = \Delta a \tag{24}$$

Since the area $\Delta V'HV$ is a right triangle, the following equations can be obtained:

$$|V'V|^2 = |V'H|^2 + |HV|^2 \tag{25}$$

$$|V'D| = R_2 \cdot sin(\alpha_1 + \beta) \tag{26}$$

$$|HD| = \sqrt{R_2{}^2 - (L/2)^2} \tag{27}$$

$$V'H = |V'D| - |HD| \tag{28}$$

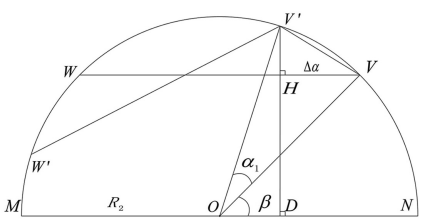

Figure 9.
The analysis model of α_1 error

$$\beta = \arcsin\left(\frac{|HD|}{R_2}\right) \tag{29}$$

The line segment $|V'H|$ can be solved by Equations from (25)–(29):

$$|V'H| = R_2 \cdot \sin\left(\alpha_1 + \arcsin\left(\frac{\sqrt{{R_2}^2 - (L/2)^2}}{R_2}\right)\right) - \sqrt{{R_2}^2 - (L/2)^2} \tag{30}$$

In the triangle $\Delta V'OV$, the line segment $|V'V|$ can be obtained from the chord length formula:

$$|V'V| = 2R_2 sin(\alpha_1/2) \tag{31}$$

The relationship among R, Δa, L and α_1 is obtained according to Equations (24), (25), (30), and (31):

$$R_2 \cdot \sin\left(\alpha_1 + \arcsin\left(\frac{\sqrt{{R_2}^2 - (L/2)^2}}{R_2}\right)\right) = \sqrt{(2R_2 \sin(\alpha 1/2))^2 - \Delta a^2} + -\sqrt{{R_2}^2 - (L/2)^2} \tag{32}$$

2.4.2 α_2 error analysis. The relationship among R, Δa, L and α_2 is established on the condition that the radius of curvature R, the robot's absolute positioning accuracy Δa and the laser displacement sensor measuring point distance L keep unchanged. As shown in Figure 10, when the error offset Δa occurs, the normal vector of the actual processing point on the surface is changed from the normal vector $\overrightarrow{OF}$ at the theoretical point to the normal vector $\overrightarrow{OF'}$ at the actual processing point. The angle between these two vectors is α_2, the radius of curvature of the circle is R_1 and the relationship can be expressed as:

$$\alpha_2 = \arcsin\left(\frac{\Delta a}{R_1}\right) \tag{33}$$

The relationship among $\Delta\theta$, ΔR, Δa and the radius R of curvature can be drawn by combining Equations (22), (23), (32) and (33), as shown in Figure 11. It can be seen that the error curve $\Delta\theta$ possesses an initial value instead of starting from the origin. The reason is that on the same curvature surface, the error offset Δa occurs when the deflection angle of the tooltip point is greater than the deflection angle of the normal vector fitted by the laser displacement sensor. Due to the relatively large radius of curvature, the above problems have little impact on $\Delta\theta$, and studies have shown that when the radius of curvature is greater than 110 mm, the impact

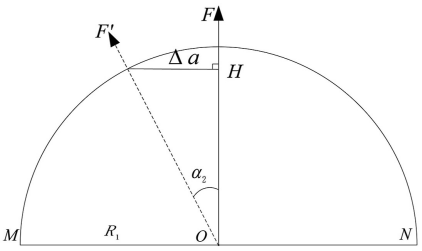

Figure 10.
The analysis model of α_2 error

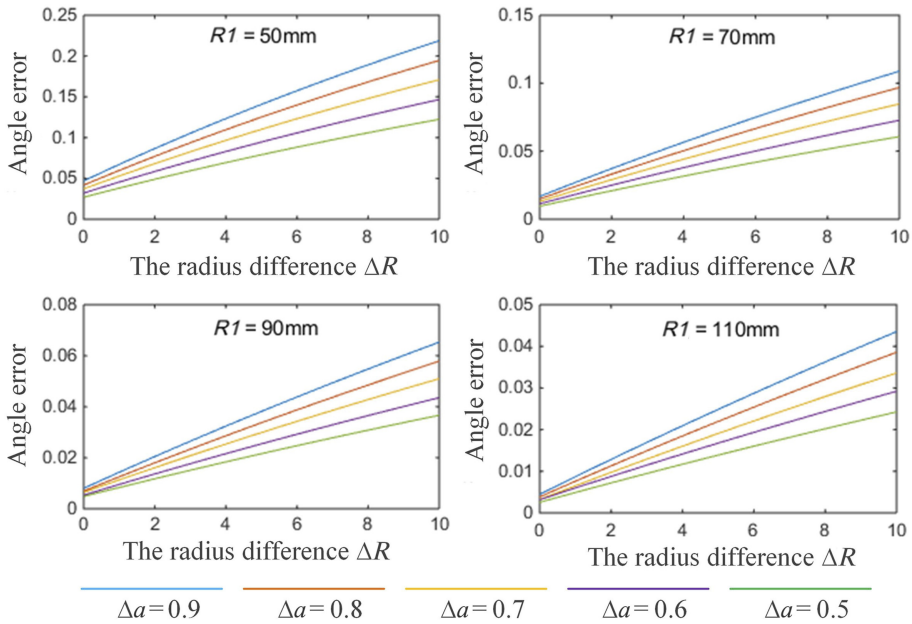

Figure 11. Relationships among $\Delta\theta$, ΔR and Δa

on $\Delta\theta$ is less than 0.005°. Thus, the effects of ΔR and Δa on $\Delta\theta$ can be ignored. Otherwise the effect of the curvature variation of the curved surface and the positioning accuracy of the robot should be considered. The growing trend of $\Delta\theta$ is directly determined by the size of Δa. In order to ensure compensation accuracy, the absolute positioning accuracy of the robot is generally controlled within 0.5 mm.

3. Experimental validation of vertical accuracy compensation method

3.1 Experimental set-ups

The offline vertical accuracy compensation is implemented in the simulation environment of DELMIA software. The calibration of four laser displacement sensors is conducted by the aforementioned plane fitting method, and the pose of the laser displacement sensors in the tool coordinate system TCP is established according to the calibration data. The digital model of the panels with variable curvature is imported in DELMIA to complete the construction of the offline simulation, as shown in Figure 12.

The validation of online vertical accuracy compensation is carried out on the robot drilling and riveting system. The API-T3 laser tracker is used as the measurement tool, and the special wing skin with variable curvature surface is used as the experimental object. The robot automatic drilling and riveting system based on laser non-contact vertical precision compensation is used as the experimental platform, as given in Figure 13.

3.2 Results and discussion for effectiveness of compensation

The offline simulation environment was constructed according to the proposed method proposed in section 2.3. First, the calibration data of the laser displacement sensor is obtained in the laser non-contact vertical accuracy compensation algorithm, or the laser displacement sensor on-site could be calibrated using the laser tracker. Based on the calibration data, the relative position relationship between the tool coordinate system and the laser displacement sensor is established

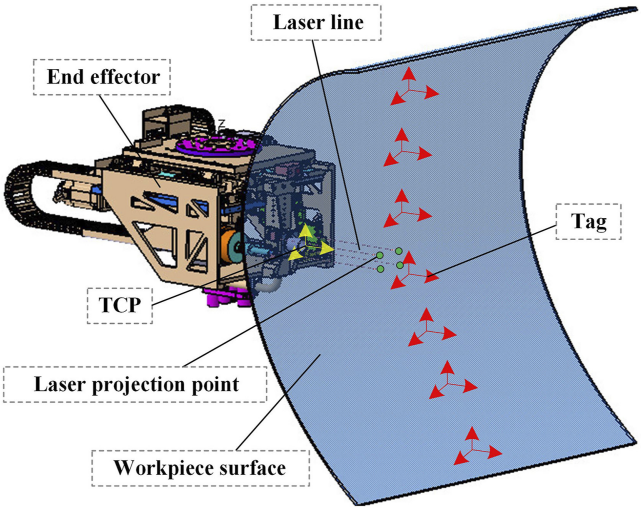

Figure 12.
Schematic diagram of simulation prediction environment

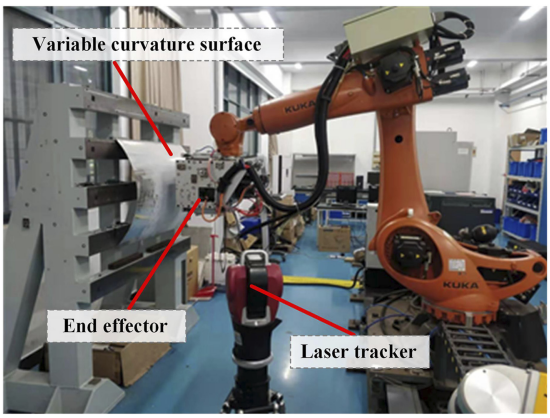

Figure 13.
The robot drilling and riveting experimental platform for vertical accuracy compensation

in the DELMIA simulation environment to complete the construction of the end effector. Secondly, the TCP of the end effector is set to coincide with the tag coordinate system of the theoretical hole on the workpiece, and the position of the intersection points between the laser lines and the workpiece surface is obtained to fit the plane and its normal vector with least square fitting method. Finally, when the angle between the X-axis of TCP and the fitting vector exceeds 0.5°, they are adjusted to coincide according to the online compensation method described in Section 2.2.2. After the simulation is complete, the angle between the X-axis of TCP and the normal vector of the theoretical hole is the inherent theoretical error, which is used as the predicted declination angle of the vertical accuracy compensation.

The theoretical error is obtained by combining the digital model of the experimental workpiece and the theoretical error prediction method proposed in this paper, and the offline programming system was used to generate NC code. The NC codes of the experimental reference points are shown in Table 1.

Before the online compensation experiment, the on-site experiment environment is set up. First, the workpiece is fixed on the tooling, and the laser tracker is used to calibrate the relative position relationship between the robot base coordinate system and the workpiece coordinate system to ensure that the robot end can correctly execute the off-line NC code. In order to detect the normal accuracy before and after off-line compensation, a laser tracker is used to measure the normal vector at the point to be measured on the curved surface. Then the normal vector of the tool axis after laser non-contact vertical precision compensation and the normal vector of the tool axis after compensation of the inherent theoretical error are measured.

The specific experimental steps are as follows: (1) The laser tracker is used to measure the normal direction of the point to be measured on the curved surface. (2) The NC code is executed to make the end effector move to the point to be measured, and the laser non-contact vertical accuracy compensation program is executed to achieve vertical accuracy compensation. (3) After laser non-contact vertical precision compensation, the spindle direction vector of the end effector is measured by the laser tracker. (4) The inherent theoretical error compensation procedure is executed for theoretical error compensation. (5) The laser tracker is used to measure the direction vector of the main axis on the end effector. During validation, the above experimental steps are repeated, and a serial set of experimental data are measured. The experimental data are shown in Tables 2 and 3.

Serial number	X (mm)	Y (mm)	Z (mm)	A (°)	B (°)	C (°)	θ_1 (°)	θ_2 (°)
1	223.483	11490.93	90.9890	90.241	11.541	180	0.012392	−0.00564
2	219.531	11418.58	120.693	90.611	7.9590	180	0.020620	0.001049
3	219.125	11253.34	123.470	90.683	8.6840	180	0.012372	0.000896
4	218.766	11139.46	125.744	90.869	9.2800	180	−0.00700	0.003745
5	222.822	11083.53	94.4170	91.854	10.304	180	0.018573	0.001190
6	224.409	10987.79	86.7500	91.728	13.079	180	0.004440	0.010617

Table 1. NC data for the off-line programming

	Surface normal vector			Spindle normal after online correction			
Serial number	i	j	k	i	j	k	Error (°)
1	0.989771	−0.00038	0.200122	0.948610	0.006720	0.316378	0.7823
2	0.990367	0.00027	0.138464	0.987296	−0.00095	0.158887	1.1830
3	0.988540	0.00054	0.150961	0.986594	−0.00086	0.163192	0.7110
4	0.986918	0.00101	0.161225	0.988453	−0.00424	0.151469	0.4550
5	0.983873	0.00042	0.178870	0.980391	−0.00098	0.197059	1.0660
6	0.974062	0.00081	0.226282	0.975130	−0.00949	0.221432	0.6500

Table 2. Surface normal vector and the normal axis of tool axis after laser non-contact vertical accuracy compensation

	Surface normal vector			Spindle normal after offline compensation			
Serial number	i	j	k	i	j	k	Error (°)
1	0.989771	−0.00038	0.200122	0.980974	0.002163	0.194128	0.368
2	0.990367	0.00027	0.138464	0.990593	0.003215	0.136802	0.207
3	0.988540	0.00054	0.150961	0.988049	−0.00425	0.154081	0.303
4	0.986918	0.00101	0.161225	0.987387	−0.00262	0.158302	0.225
5	0.983873	0.00042	0.178870	0.984949	−0.00016	0.172842	0.349
6	0.974062	0.00081	0.226282	0.974168	−0.00590	0.225746	0.326°

Table 3. Surface normal vector and tool axis normal vector after compensating inherent theoretical error

From the data in Table 2, it can be seen that the laser non-contact normal measurement method has a large measurement error for the variable curvature surface, generally exceeding 0.5°, which cannot meet the assembly precision of vertical precision of drilling during aircraft assembly. It can be seen from the data in Table 3 that the vertical accuracy compensation method of the variable curvature surface proposed in present research can limit the error within 0.4° after theoretical error compensation.

4. Conclusions

In the present research, a combined vertical accuracy compensation method for automatic drilling and riveting of aircraft panels with variable curvatures is proposed and validated in a robot drilling and riveting system. The findings and conclusions can be summarized as follows:

(1) The proposed vertical accuracy compensation method combines online calibration and offline prediction. The former is aimed to correct the vertical error between actual and theoretical riveting positions based on laser ranging, and the latter is to correct the vertical error caused by the approximate plane fitting in variable-curvature panels based on model curvature.

(2) The combined vertical accuracy compensation method is applied in an automatic robot drilling and riveting system. The verticality error can be controlled within 0.4° when the proposed method is used to compensate for the vertical accuracy of the variable curvature surface, which can meet the requirement of the aerospace manufacturing industry for vertical accuracy.

(3) The normal vector predication error in offline compensation method caused by the absolute positioning accuracy of the robot is elaborately analyzed. The compensation accuracy could be guaranteed when the absolute positioning accuracy of the robot is generally controlled within 0.5 mm.

References

Alici, G. and Shirinzadeh, B. (2005), "A systematic technique to estimate positioning errors for robot accuracy improvement using laser interferometry based sensing", *Mechanism and Machine Theory*, Vol. 32, pp. 105-212.

Cao, J.J., Chen, H., Zhang, J., Li, Y.J., Liu, X.P. and Zou, C.Q. (2018), "Normal estimation via shifted neighborhood for point cloud", *Journal of Computational and Applied Mathematics*, Vol. 329, pp. 57-67.

DeVlieg, R., Sitton, K., Feikert, E. and Inman, J. (2002), "ONCE (one-sided cell end effector) robotic drilling system", *SAE Technical Paper*, Vol. 26, pp. 20-38.

Gao, Y.H., Wu, D., Dong, Y.F., Ma, X.G. and Chen, K. (2017), "The method of aiming towards the normal direction for robotic drilling", *International Journal of Precision Engineering and Manufacturing*, Vol. 18, pp. 787-794.

Hogan, S., Hartmann, J., Thayer, B., Brown, J., Moore, I., Rowe, J. and Burrows, M. (2003), "Automated wing drilling system for the A380-GRAWDE", *SAE Aerospace Automated Fastening Conference and Exhibition-2003 Aerospace Congress and Exhibition*, pp. 1-8.

Hu, J.S., Sun, X.Y., Tian, W., Xuan, S.Y., Yan, Y., Wang, C.R. and Liao, W.H. (2022), "A combined hole position error correction method for automated drilling of large-span aerospace assembly structures", *Assembly Automation*, Vol. 42, pp. 293-305.

Jin, J., Tian, W., Hu, J.S., Ge, C.T., Qian, X.S. and Liao, W.H. (2022), "An efficiency and quality based automatic drilling-riveting system for aero-structures assembly", *Proceedings of the Institution of Mechanical Engineers, Part B: Journal of Engineering Manufacture*.

Lee, R.T. and Shiou, F.J. (2010), "Calculation of the unit normal vector using the cross-curve moving mask method for probe radius compensation of a freeform surface measurement", *Measurement*, Vol. 43, pp. 469-478.

Lee, R.T. and Shiou, F.J. (2011), "Multi-beam laser probe for measuring position and orientation of freeform surface", *Measurement*, Vol. 44, pp. 1-10.

Li, M., Tian, W., Hu, J.S., Wang, C.R. and Liao, W.H. (2022), "Effect of hole perpendicularity error and squeeze force on the mechanical behaviors of riveted joints", *Microscopy Research and Technique*, Vol. 85, pp. 1075-1088.

Mei, B., Zhu, W.D. and Ke, Y.L. (2018), "Positioning variation analysis and control for automated drilling in aircraft manufacturing", *Assembly Automation*, Vol. 38, pp. 412-419.

Olsson, T., Haage, M., Kihlman, H., Johansson, R., Nilsson, K., Robertsson, A., Björkman, M., Isaksson, R., Ossbahr, G. and Brogårdh, T. (2010), "Cost-efficient drilling using industrial robots with high-bandwidth force feedback", *Robotics and Computer-Integrated Manufacturing*, Vol. 26, pp. 24-38.

Prakash, R.U., Kumar, G.R., Vijayanandh, R., Kumar, M.S. and Ramganesh, T. (2016), "Structural analysis of Aircraft fuselage splice joint", *IOP Conference Series: Materials Science and Engineering*, Vol. 149, pp. 1130-1137.

Rummell, T. (2000), "The evolution of all electric fastening systems G86 to multi-flex", *SAE Transactions*, Vol. 109, pp. 755-758.

Su, Z., Rosell, A., Udpa, L. and Tamburrino, A. (2017), "February. Model-based study for evaluating the sensitivity of eddy current GMR probe inspection of multilayer structures", *AIP Conference Proceedings*, Vol. 1806, 110016.

Tian, W., Zhou, W., Zhou, W., Liao, W. and Zeng, Y. (2013), "Auto-normalization algorithm for robotic precision drilling system in aircraft component assembly", *Chinese Journal of Aeronautics*, Vol. 26, pp. 495-500.

Wang, D., Bai, Y. and Zhao, J. (2010), "Robot manipulator calibration using neural network and a camera-based measurement system", *Transactions of the Institute of Measurement and Control*, Vol. 32, pp. 105-121.

Zhang, L., Tian, W., Li, D.W., Hong, P., Li, Z.Y., Zhou, W.X. and Liao, W.H. (2018), "Design of drilling and riveting multi-functional end effector for CFRP and aluminum components in robotic aircraft assembly", *Transactions of Nanjing University of Aeronautics and Astronautics*, Vol. 35, pp. 529-538.

Corresponding author
Junshan Hu can be contacted at: hujunshan@nuaa.edu.cn

For instructions on how to order reprints of this article, please visit our website:
www.emeraldgrouppublishing.com/licensing/reprints.htm
Or contact us for further details: **permissions@emeraldinsight.com**